IMPLICATIONS OF STERIC CONGESTION ON SHEET FORMATION: 26-ATOM MACROCYCLES

by

Lola C. Kouretas

Submitted in partial fulfillment of the

requirements for Departmental Honors in

the Department of Chemistry and Biochemistry

Texas Christian University

Fort Worth, Texas

May 6, 2024

IMPLICATIONS OF STERIC CONGESTION ON SHEET FORMATION: 26-ATOM MACROCYCLES

Project Approved:

Supervising Professor: Eric Simanek, Ph.D.

Department of Chemistry and Biochemistry

Jean-Luc Montchamp, Ph.D.

Department of Chemistry and Biochemistry

Antoinette Denapoli, Ph.D.

Department of Religion

ABSTRACT

Molecular engineering of large macrocyclic compounds offers new avenues to disrupt protein-protein interfaces and potentially halt pathways that lead to neurodegenerative diseases such as Alzheimer's. The hallmark of Alzheimer's disease involves the aggregation of so-called amyloid peptides that exhibit characteristic β-sheet structures. Thus, designing macrocycles that structurally/topologically mimic β-sheets should enhance the affinity of these macrocycles towards the amyloid aggregates and lead to rational design of more advanced scaffolds with therapeutic potential. These scaffolds could potentially present opportunities to interfere with protein-protein interactions, thus preventing amyloid plaque formation.

This work will describe the synthesis of structurally- and functionally-diverse macrocyclic scaffolds to understand the factors that contribute to β-sheet formation. Here, 26-atom macrocycles prepared in three-steps will be described. Using a triazine core, a protected hydrazine group and an acetal on an amino acid tether, a monomer can be prepared in two steps. Acetals ranging from 2-4 carbons can be used to yield rings of 22-28 atoms. Treatment with acid leads to dimerization in very high yields. Varying the amino acid choice can lead to synthesis of different homodimers and heterodimers. Previous work proves acetal length dictates morphology; three-carbon acetals give folded conformations and five-carbon acetals yield crinkled β-sheets. Four-carbon acetals yield the flattened β -sheets described here. NMR spectroscopy provides confirmation of synthesis and 2D-NMR techniques offer opportunities to probe solution structure more efficiently. Intramolecular hydrogen bonding within the template exhibited by 1D-NMR may corroborate the belief that that these macrocycles adopt a β-sheets like structure.

ACKNOWLEDGEMENTS

I want to convey my sincere gratitude and appreciation for the individuals involved in the making of this thesis and my overall research experience. The professors within the department of Chemistry and Biochemistry have given me the tools needed to become an independent and skilled researcher capable of creating a thesis I am proud of. To Dr. Eric Simanek, thank you for your patience in answering all my questions for two years and in pushing me to become an adept scientific writer, confident presenter, and curious researcher. Your dedication towards helping me succeed in your lab and in making my dreams a reality by applying to graduate school (Go Aggies!) is something I will never forget. To all of the other graduate and undergraduate students in the Simanek lab, I thank you for the support and strong camaraderie we have built. I would like to specifically acknowledge Gretchen Pavelich for her synthesis contribution in this thesis. I also want to extend my thanks to Drs. Kayla Green and Sergei Dzyuba for their pivotal guidance in editing and perfecting my graduate school application materials. Thank you to Dr. Jean-Luc Montchamp for serving on my committee along with Dr. Antoinette Denapoli. I would also like to acknowledge the John V. Roach Honors college and funding sources such as the National Institutes of Health (grant R15GM135900) and the Robert A. Welch Foundation that have supported my research financially. Lastly, thank you to my best friends and my family for showing me unwavering love, kindness and support in every facet of my life. It does not go unnoticed.

TABLE OF CONTENTS

TERMINOLOGY & ABBREVIATIONS

Abbreviation	Full term
BOC	*tert*-butyloxycarbonyl
BRo5	beyond rule of 5
COSY	homonuclear correlation spectroscopy
DCM	dichloromethane
DIPEA	diisoproylethylamine
DMA	dimethylamine
DMSO	dimethylsulfoxide
H	hydrogen
HBTU	hexfluorophosphate benzotriazole tetramethyl uronium
MeOH	methanol
MeOH-d_4	deuterated methanol
NMR	nuclear magnetic resonance

NOE	Nuclear Overhauser Effect
PPI	Protein-Protein Interaction
ppm	parts per million
ROESY	Rotating Frame Overhauser Effect Spectroscopy
TLC	Thin-Layer Chromatography

FIGURES & SCHEMES

INTRODUCTION

Macrocyclic drugs are of interest because of their ability to inhibit biomolecular interactions that conventional small molecules cannot access.[1] The design of small molecule drugs involves protein-ligand interactions because protein receptors usually contain a small, easily identifiable ligand-binding site that small molecules can engage with.[2] While successful, this paradigm is only one way to combat disease and is limited to protein targets that have a complementary ligand.

Intracellular protein-protein interactions (PPIs) are of interest because they play essential roles in biological processes; undesirable PPIs are linked to cancer, neurodegenerative and infectious diseases. Over the recent decades, targeting PPIs has been acknowledged as one of the most formidable challenges in drug discovery because these interfaces tend to be flat and contains few grooves or pockets, making it challenging for complementary small molecule ligands to bind.
Large molecule therapeutics act on PPIs by increasing the number of interactions by maximizing the surface contacts. These therapeutics possess a larger molecular weight molecular weight (>500 Da), posing challenges in meeting criteria such as Lipinski's "rule of 5" (Ro5).[2] Further, since most PPIs lack endogenous small molecule ligands, it is difficult to rationally design complementary PPI modulators.

Macrocyclic drugs can be explored as a modality for inhibition of PPIs for numerous reasons.[3] First, macrocycles are 3-5 times larger than traditional small-molecule drugs and contain binding surfaces similar in size to native PPI interfaces. Macrocycles can adopt multiple conformations ─a behavior referred to as chameleonicity ─ to navigate hydrophobic cellular membranes and aqueous

intracellular environments. This characteristic affords advantages where the macrocycle can assume either extended conformations that facilitate PPI binding or folded structures that boost hydrophobicity to promote membrane permeability.[4]

Lipinski's Ro5 outlines guidelines for optimizing passive membrane permeability and achieving sufficient oral bioavailability when designing large molecules. Empirical guidance suggests that a molecular weight of ≤500, ≤5 hydrogen bond donors, ≤10 hydrogen bond acceptors, and an octanol-water partition coefficient (LogP≤5) are favorable characteristics. [3] Drugs beyond the rule of 5 (bRo5) such as macrocycles derive largely from nature and are not the historic targets of the pharmaceutical industry. While their higher pharmacokinetic risks (low solubility and permeability) are the Achilles heel of this class of compounds, the synthetic community continues to investigate these molecules to expand the pool of potential drug leads.[5]

The molecular complexity and range of structural modifications that macrocycles can tolerate make them interesting. They can be engineered to have restricted internal bond rotations, limiting the number of conformations accessible which lowers the entropic cost upon binding of the macrocycle to its target.[6] One way to ensure a specific bioactive conformation is to alter ring size. The effect of 14- to 16- membered macrocycles on CHK1 potency is an example; computational analysis of these molecules revealed larger 16-membered rings showed reduced affinity for the target which could be attributed to the greater flexibility and extended conformation of the macrocycle. [7] It is clear that the potency of macrocycles as inhibitors can be retained or improved by manipulating the scaffold and varying the size of macrocyclic backbone.

Macrocycles have gained traction as inhibitors of biological processes associated with neurodegenerative diseases, such as Alzheimer's.[8] Extracellular amyloid plaques formed by antiparallel-layered β-sheets are the most visible evidence of Alzheimer's progression.[9] Designing and tailoring a molecular scaffold to mimic amyloid fibril β-sheets could provide insight into both amyloid oligomers and the aggregation process in general. Professor James Nowick pioneered the idea of using macrocyclic β-sheet peptides to inhibit the aggregation of a tau-protein-derived peptide. He designed a series of macrocycles where the "upper" strand can delay and suppress the onset of aggregation of a β-sheet peptide. The amino acid residues in the lower strand give a pattern of hydrophobicity and hydrophilicity that match the upper strand of the peptide, allowing for binding and thus inhibition of stacking of sheets. Herein, I present a different approach that suggests a 26-atom triazine macrocycle could serve as a β-sheet mimic (and potential inhibitor of amyloid fibril aggregation in the long term).

This research is anchored by an earlier study exploring the structure of 22-28 atom macrocycles using crystal structure data. [11] The x-ray structure of a 26-atom glycine macrocycle (**figure 1** below) shows an extended, flat structure instead of a partially or fully folded conformation seen in other macrocycles (which resembles the flat conformation of β-sheets.)

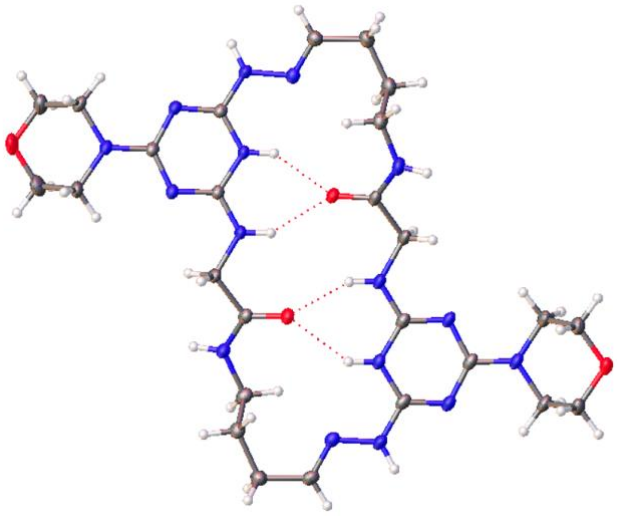

Figure 1. Crystal structure of 26-atom **G-G** macrocycle from the top. The dotted lines indicate a network of intramolecular hydrogen bonds that promotes macrocyclization.

The route for preparation of 26-atom macrocycles is shown in Scheme 1. It involves a step-wise synthesis of a triazine core with an amino acid, hydrazine protecting group and auxiliary group (dimethylamine) to afford an acid intermediate (**I-**acid below). The amino acid can then be activated using coupling reagents to add a four-carbon diethyl acetal. This affords monomer **I**. Acid-catalyzed deprotection is used to afford the macrocycle **I-I** from the monomer.

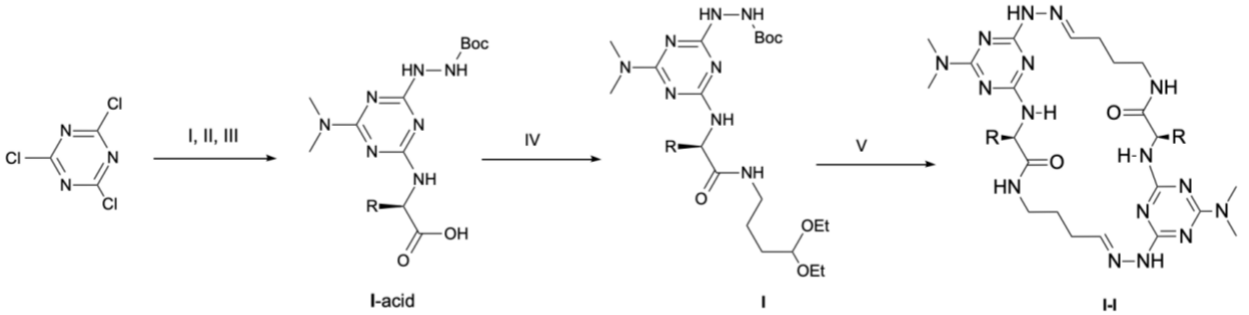

Scheme 1. Synthesis route to afford a macrocycle containing isoleucine. I) BOC-hydrazine, NaOH (aq), THF. II) Isoleucine. III) Dimethylamine. IV). DIPEA, HBTU and 1-amino-4,4-diethoxyamine. V) 1 DCM : 1 TFA.

Although Scheme 1 shows the synthesis of a macrocycle from two identical monomers, this thesis also investigates a heterodimer containing isoleucine (**I)** and methionine (**M)** to yield **I-M** in addition to **I-I**. The choice of amino acid is deliberate; isoleucine is a β-branched amino acid and is hydrophobic and offers the opportunity to probe steric tolerances.[4] Further, the inclusion of two hydrophobic amino acids may be useful in synthesizing a β-sheet mimic. The hydrophobic exterior surfaces of β-sheets will self-assemble through hydrophobic interactions to form aggregates. [13] To interrupt β-sheet stacking that forms aggregates, β-sheet mimics should include hydrophobic residues. These residues can also boost membrane permeability by increasing hydrophobicity. [14]

Previous research of 24-atom macrocycles have identified the existence of isomers of **I-I** that derive from the epimerization of the α-carbon in the amino acid; one macrocycle preserves (S,S) stereochemistry, and the other (R,S). The diastereosiomers of this macrocycle exhibit unique resonances in the ^{1}H NMR spectrum, which can also be seen in the spectrum of the 26-atom **I-I**. The appearance of isomers will be discussed in this work. Two types of 2D NMR experiments will

be explored: correlation spectroscopy (COSY) and nuclear Overhauser effect spectroscopy (NOESY).[15] COSY experiments provide correlations between neighboring protons to characterize molecules and prove synthesis. Through-space experiments correlate protons that are far apart in the macrocycle but are close in three-dimensional space; these protons will have an nOe signal. A rotating frame Overhauser enhancement spectroscopy experiment (ROESY) is a type of nOe experiment used in this thesis to probe possible conformations of the macrocycles in solution state. In solution, our macrocycles may present rOe's that are only possible if the molecule adopts a folded conformation. The absence of these signals may provide evidence for a flat conformation reminiscent of a β-sheet structure. The culmination of findings from 1D and 2D NMR spectra are e utilized to comment on the ability of the 26-atom macrocycle scaffold to serve as a β-sheet mimic.

EXPERIMENTAL

NMR Spectroscopy. Room temperature NMR spectra were recorded with a 400 MHz Bruker Avance spectrometer. All chemical shifts in the ^{1}H spectra were calibrated according to a corresponding residual solvent resonance (e.g. DMSO-d6, = 2.52 ppm) in parts per million. All 2D spectra were taken also taken on the 400 MHz Bruker Avance relative to corresponding solvent resonances. NMR solvents used were all deuterated and purchased as ampules.

General Chemistry. Thin-later chromatography (TLC) experiments were carried out in a sealed container on silica plates with a pore size of 60Å, a particle size of 50-63 m, surface area of 500-600 m^2/g, a bulk density of 0.4 g/mL and a pH range of 6.5-7.5. TLC results were visualized on the silica plate using ultraviolet light (UV) and by staining with ninhydrin (1.5 g ninhydrin in 100 mL of *n*-butanol and 3.0 mL acetic acid) followed by heating to identify the presence of a

primary/secondary amine. Column chromatography experiments were carried out on silica gel (Silicycle) with a porosity of 60Å, particle size of 50 to 63 μm, surface area of 500 to 600 m^2/g, a bulk density of 0.4 g/mL, and a pH range of 6.5 to 7.5. Either Dichloromethane/methanol or hexanes/ethyl acetate were used as the eluent for chromatographic purification. Excess solvents were removed using rotary evaporation on a Buchi Rotovapor RII with a Welch Self-Cleaning Dry Vacuum System. All workup and purification procedures were conducted with reagent-grade solvents under an ambient atmosphere.

*Macrocycle **I-I.*** Monomer **I** (68.5 mg) was dissolved in 1 mL dichloromethane in a 3 mL vial containing a mini stir bar. Trifluoroacetic acid (1 mL) was added dropwise via pipette. Evaporation occurred over the course of 14 days in the uncapped vial. The resulting brown oil was analyzed using ^{1}H NMR to characterize and assess purity. ^{1}H NMR (DMSO-d_6, 400 MHz): δ 12.4 (s, 1H), 11.7 (m, 1H), 8.2 (m, 1H), 7.8 (m, 2H), 7.6 (s, 1H), 4.6 (m, 1H), 4.5 (s, 1H), 3.1 (m, 6H), 2.8 (m, 1H), 2.7 (m, 1H), 2.3 (m, 1H), 2.0 (m, 1H), 1.8 (m, 1H), 1.4 (m, 1H), 1.2 (m, 4H), 0.9 (m, 6H). ^{13}C{1H} NMR (DMSO-d_6, 100 MHz): δ 159.4, 159.0, 158.6, 158.3, 120.3, 117.4, 114.5, 111.7, 111.6, 38.1, 37.1, 29.5, 26.1, 24.3, 16.0, 15.1, 12.1, 11.9.

*Macrocycle **I-M.*** Monomer **I** (13.4 mg) was dissolved in 1 mL DCM in a 3mL vial containing a mini stir bar. A methionine containing monomer (**M**) synthesized by Gretchen Pavelich was dissolved in DCM and added to the vial. Trifluoroacetic acid (1 mL) was added dropwise via pipette. Evaporation occurred over about 8 days to give a brown oil. ^{1}H NMR (DMSO-d_6, 400 MHz): δ 12.4 (s, 1H), 11.5 (s, 1H), 8.9 (s, 1H), 8.5 (s, 1H), 7.9 (s, 3H), 7.6 (s, 1H), 4.7 (m, 1H),

4.6 (m, 1H), 4.0 (m, 1H), 2.5 (m, 1H), 2.3 (m, 2H), 2.0 (m, 1H), 1.8 (m, 2H), 1.4 (m, 1H), 1.2 (m, 4H), 0.9 (m, 3H). No $^{13}C\{1H\}$ NMR was obtained.

*Monomer **I**.* Intermediate **I**-acid was dissolved in 5 mL DCM in a 25 mL round bottom flask stirring at room temperature to yield a pale yellow solution. In order, DIPEA (28.8 mg, 0.22 mmol), HBTU (13.2 mg, 0.10 mmol) and 4,4-diethoxybutyl-1-amine (15.8 mg, 0.10 mmol) were added neat via pipette. The reaction progress was monitored using thin layer chromatography (10% MeOH in DCM); after 24 hours, the single spot starting material (R_f = 0.7) had disappeared, and a new spot at R_f = 0.5 was observed under short wave UV irradiation. The solution was then rotovapped to eliminate extra solvent, dissolved in ethyl acetate and extracted with three 30 mL portions of H_2O. The organic layer was dried using magnesium sulfate and filtered via gravity filtration. Column chromatography (10% MeOH in DCM) was used to further purify **I** and yield 81% of pure material. ^1H NMR (DMSO-d_6, 400 MHz): δ 8.5 (s, 1H), 8.2 (s, 1H), 7.7 (s, 1H) 6.3 (m, 1H). 4.4(m, 1H), 4.2 (m, 1H), 4.1(m, 1H), 3.5 (m, 2H), 3.3 (m, 2H), 3.0 (m, 6H), 1.5 (m, 2H), 1.4 (m, 9H), 1.2 (m, 3H), 1.1 (m, 8H), 0.9 (m, 7H). No $^{13}C\{1H\}$ NMR was obtained.

*Intermediate **I**-acid.* Cyanuric chloride (0.256 g, 1.34 mmol) was added rapidly as a solid to a stirring 50 mL round bottom flask containing 3 mL THF previously cooled using a dry ice and acetone bath. A 3 mL solution of BOC-hydrazine (0.184 g) in 3 mL THF was added dropwise over 5 minutes using an addition. The solution turned a pale yellow during this addition. After the addition was complete, 1 mL of 1 M NaOH was added over 1 minute via pipette. After one hour, thin layer chromatography (10% MeOH in DCM) showed the appearance of a single UV active spot (Rf = 0.7) that stained yellow using ninhydrin. A solution of isoleucine (0.37 g) in 1 mL H2O

and 3 mL of 1 M NaOH was then added dropwise over 2 min while. The solution started a pale yellow and turned bronze in color. The pH of the reaction mixture was 8-9 after this addition. The next day, thin layer chromatography (10% MeOH in DCM) showed appearance of a new spot at R_f = 0.05 and disappearance of starting material at R_f = 0.7, confirming the reaction was complete. The third substitution of cyanuric chloride was done by adding an aqueous solution of dimethylamine (40%, 0.4275 g by vol.) dropwise over three minutes. Immediately following addition, the solution was measured to be pH = 9. The reaction stirred for about 4 hours before thin layer chromatography (10% MeOH in DCM) showed a new spot at less than R_f = 0.25. The reaction was then acidified to pH = 5.0 with 1M HCl and extracted three times with ethyl acetate and brine. Column chromatography (7.5% MeOH in DCM) was performed and a white solid (81% yield total**)** was afforded. ^{1}H NMR (MeOD-d_4, 400 MHz): δ 4.5 (m, 1H), 3.1 (m, 6H), 2.1 (s, 2H), 1,4 (m, 9H), 0.9 (m, 6H). No ^{13}C{1H} NMR was obtained and mass spectra results are pending.

RESULTS & DISCUSSION

NMR Spectrum Conventions and Nomenclature. **Chart 1** shows conventions used for identifying NMR resonances.

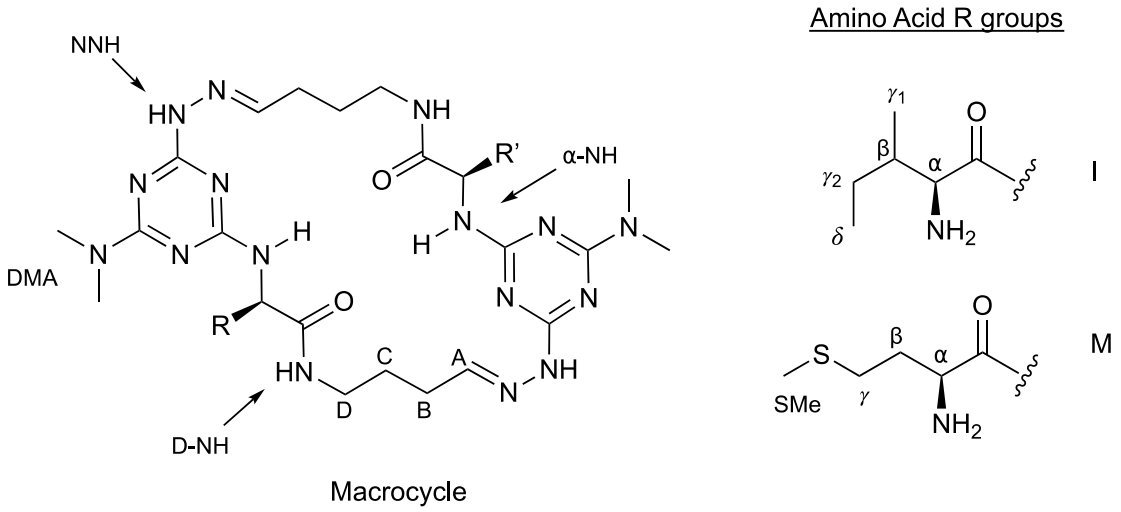

Chart 1. Labeling convention for protons in the macrocycle and in incorporated amino acid side chains.

The labeling scheme in identifies protons that will exhibit NMR signals in a spectrum. Signals from protons that are to the left of the spectrum are referred to as "upfield" and signals to the right are "downfield." Protons will be shifted downfield if they are influenced by nearby electron-withdrawing groups or electronegative atoms. Letters A, B, and C and D identify the protons attached to the four carbons on the acetal. Protons associated with D will appear most downfield because of their proximity to the electron-withdrawing amine of the acetal (D-NH). In the monomer spectra, the ethoxy groups of acetal are denoted as "acetal CH_3" or "acetal CH_2" when appropriate. The DMA label denotes the dimethylamine auxiliary group. NNH is used to represent the proton attached to the hydrazine NH. The α-NH represents the amino acid amine. R and R' represent the R groups in the amino acids isoleucine **(I)** and methionine **(M)**. In the spectra of **I**-acid and **I**-Monomer, the protecting group *N*-BOC-hydrazine is used to identify the *tert-butyl* group on the hydrazine. In the macrocycle spectrum, the H^+ refers to the proton present when the

triazine ring is protonated under acidic conditions. This labeling system in **Chart 1** is conserved across all intermediates and macrocycle NMR signals in the ^{1}H spectra.

Part I. Synthesis and Characterization of Monomer I

*Synthesis of Intermediate **I**-acid.* The synthesis of acid intermediates takes advantage of a stepwise substitution of cyanuric chloride. First, *N*-BOC-hydrazine is added followed by the appropriate amino acid, and finally dimethylamine. These substitutions proceed through nucleophilic aromatic substitution where the chlorine can be easily displaced by an incoming nucleophile, such as the amine of the hydrazine. The order of addition is largely dictated by the reactivity of the nucleophiles and solubility of the resulting intermediate dichlorotriazine intermediate. BOC-hydrazine is added first; this protecting group is not susceptible to hydrolysis under basic conditions and is resistant to many nucleophiles. This group is also thermally stable and soluble in many organic solvents, thus increasing the solubility of mono and dichlorotriazine intermediates when a hydrophobic amino acid such as isoleucine is added.[16] The high reactivity of the hydrazine can offer di- and tri-substituted side products, so addition occurs dropwise at 0 ℃. Next, an aqueous solution of isoleucine is added at room temperature. Adding 1M NaOH to this solution helps solubilize the amino acid and increases the rate of substitution by increasing the nucleophilicity of the amine. A target pH of 6-8 is maintained by adding another equivalent of base to ensure the amine is not present in its non-nucleophilic protonated form. Aqueous dimethylamine (40%) is added finally in excess.

The first three substitutions are carried out in the same flask and monitored using thin-layer chromatography. Isolation of **I**-acid from excess reagents and unwanted side products involves

extraction and chromatography. Column chromatography only led to partial purification, where TLC showed contamination by a faint impurity at an R_f directly above the product. The net yield of **I**-acid recovered, pure and impure, was 43%. Low product yield can most likely be attributed to loading too much volume onto the column and failing to elute all product off the column. Purification was immediately followed by NMR spectroscopy to verify successful synthesis of **I**-acid (**Figure 2).**

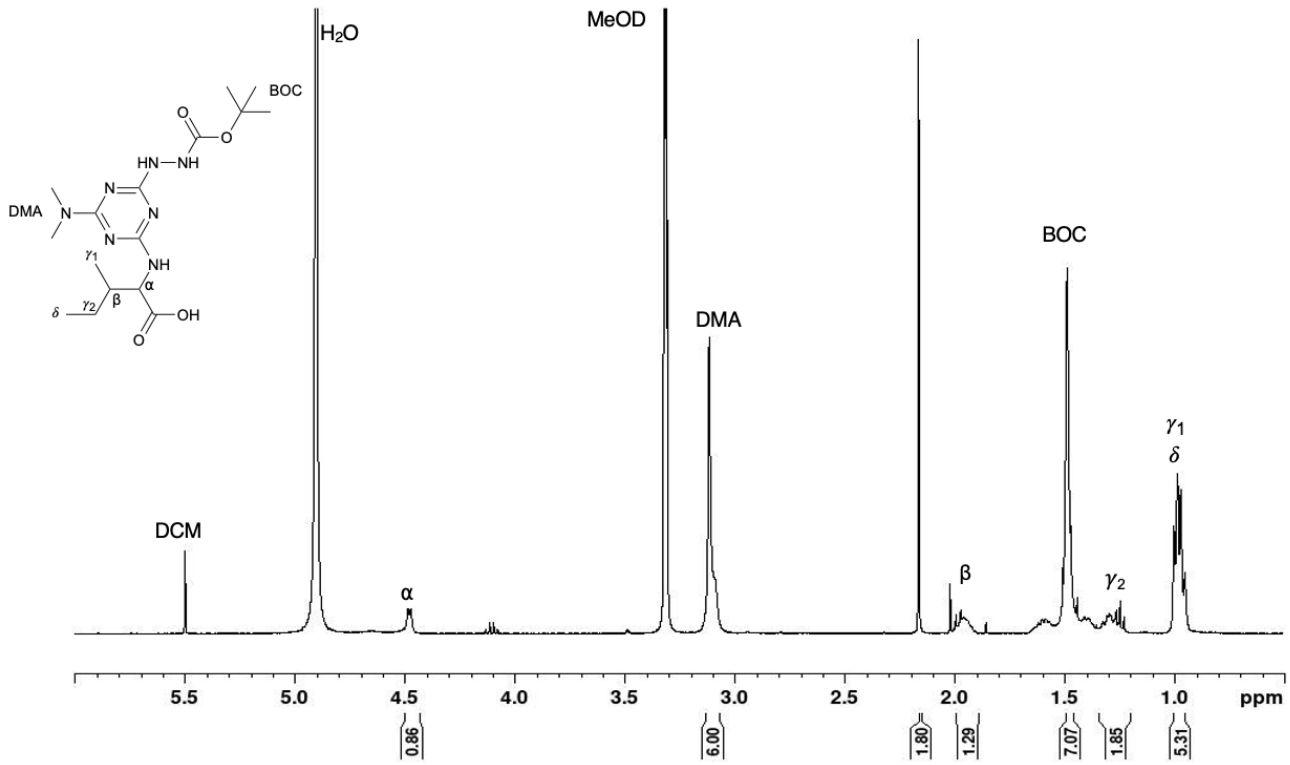

Figure 2. The 400 MHz ^{1}H NMR spectrum of **I**-acid in MeOD-d_4.

The ^{1}H NMR in **Figure 2** shows well-resolved resonances from each substitution such as BOC-hydrazine, isoleucine and DMA. The amino acid side chain resonances from 0.95 to 2.02 ppm (β, γ_1, γ_2 and δ) as well as the α hydrogen at 4.49 ppm verify successful substitution of isoleucine. DMA appears at 3.11 ppm and the BOC group at 1.48 ppm.

*Synthesis of Monomer **I.***

Following successful synthesis of **I**-acid, a diethylacetal group replaces the carboxylic acid of isoleucine using coupling agent HBTU. The acetal group can serve as the amino acid tether, where varying the length can alter the ring size of the macrocycle. Acid hydrolysis of this functional group can facilitate hydrazone formation. Excess HBTU can be used to couple amino acids in peptide synthesis by activating the carboxylic acids and forming a stable leaving group that can be replaced with an incoming amino acid to form the desired amide. Similarly, in this research, an amine (4,4-diethoxybutylamine) containing terminal acetal groups can replace the acid to form an amide using HBTU. TLC is used to confirm all starting material is consumed and upon extraction and chromatography, a 34% yield of **I** is obtained. Proof of synthesis is obtained from the ^{1}H spectrum in DMSO-*d*$_6$ (**Figure 3).**

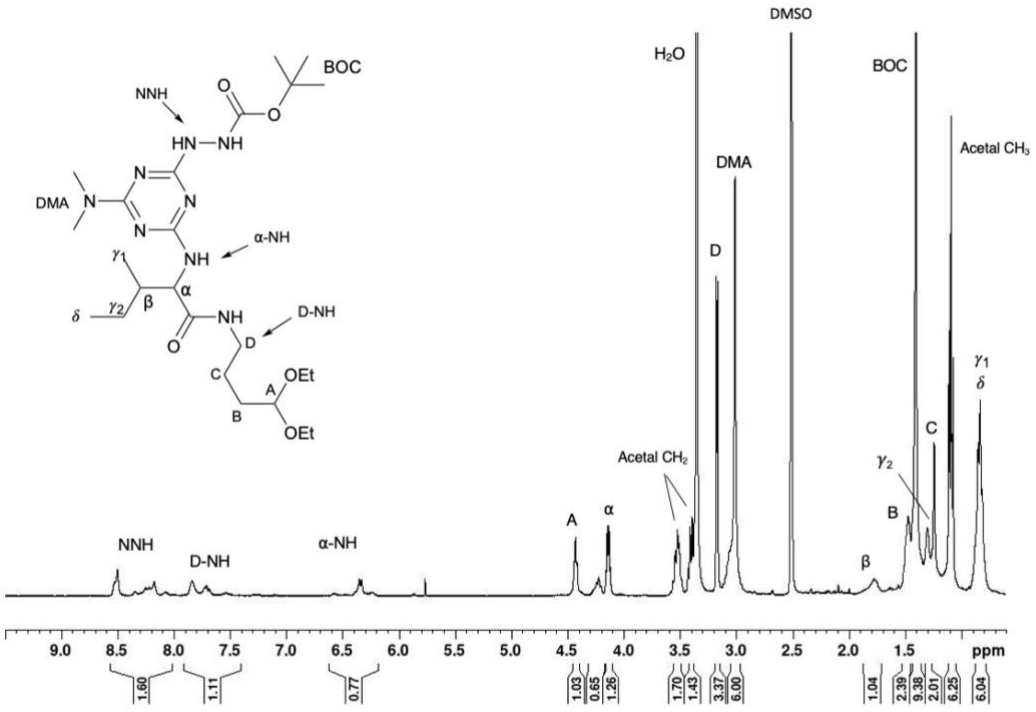

Figure 3. The 400 MHz ^{1}H NMR spectrum of **I** in DMSO-*d*$_6$. The appearance of rotamers must be noted as exhibited by the appearance of multiple resonances for a single proton.

The ^{1}H NMR in **Figure 3** is confirms the synthesis because of the appearance of new peaks corresponding to the diethylacetal group. The acetal CH_3 protons can be observed at 1.09 ppm where they split the signal into a triplet. The methylene CH_2 protons of the ethyl groups are magnetically non-equivalent, where two quartets integrate for two distinct protons with different shifts. These diastereotopic hydrogens appear at 3.40 and 3.52 ppm. These peaks coupled with the presence of A through D prove that incorporating of the acetal group onto **I-**acid to form **I** was successful. This spectra is interesting because it showcases the existence of multiple resonances for most signals. For instance, there is only one α proton in isoleucine, but there are at least two corresponding resonances. The same is true for α-NH, D-NH and NNH. These resonances are attributed to the presence of rotational isomers arising from hindered rotation about the triazine-*N* bond. It is clear that these isomers interconvert at a slow enough on the NMR timescale that distinct conformations can be detected.

Part II. Synthesis and Characterization of Homodimer Macrocycle

I-I *macrocycle.* Dimerization of two identical **I** monomers occurs in quantitative yields upon acid-catalyzed deprotection. An initial concentration of 68.5 mg/mL of **I** is dissolved in a 1:1 mixture of DCM to TFA and evaporated to dryness. The procedure affords **I-I** without the need for further purification**.** The simplicity of the resulting ^{1}H NMR spectrum of **I-I** (**figure 4)** validates successful synthesis. The acetal CH_3 and acetal CH_2 protons from the diethylacetal group are no longer present. The fingerprint region of the ^{1}H NMR spectrum of **I-I** from 7 to 13 ppm is particularly useful for characterizing the macrocycle (**figure 4).**

The presence of isomers can also be observed in **figure 4.** One-dimensional NMR offers support for the existence of two distinct macrocycles that result from racemization of the α-stereocenter. Many resonances appear twice and suggest a 50:50 mixture of the two macrocycles.

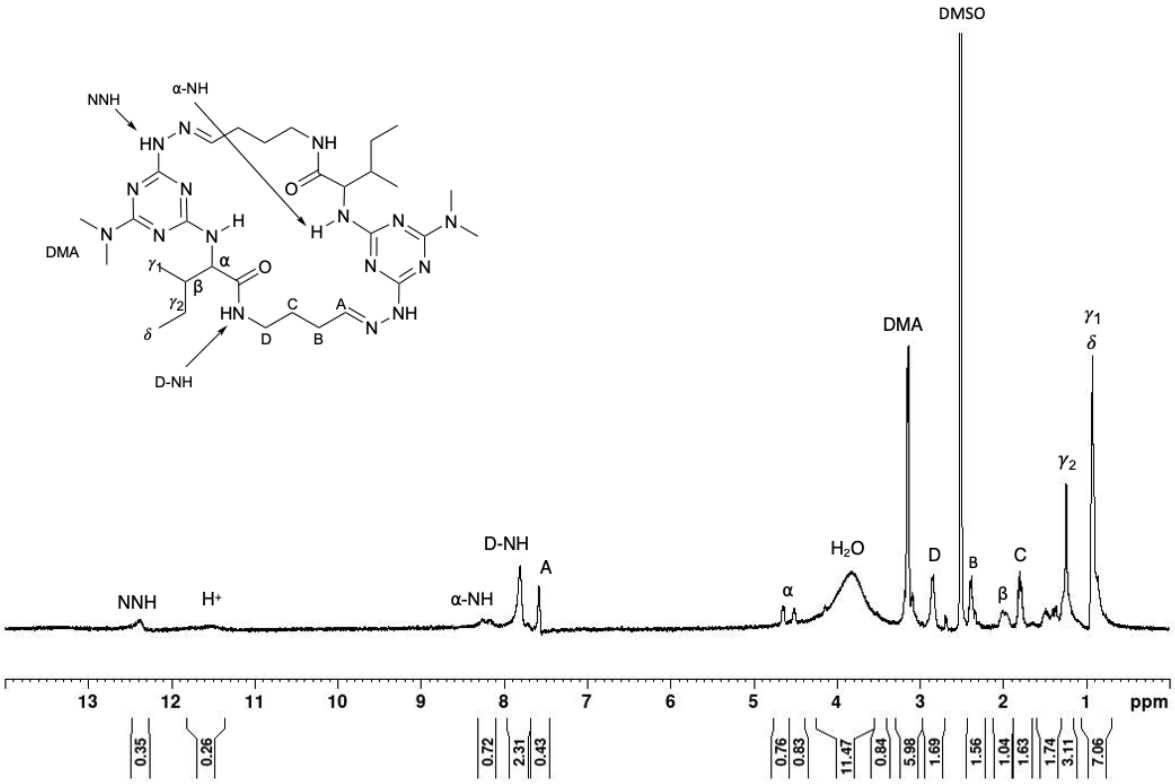

Figure 4. The 400 MHz ^{1}H NMR spectrum of **I-I** in DMSO-*d*$_6$.

The downfield shift of resonances in **figure 4** compared to **figure 3** can give insight into the conformation of **I-I**. The α-NH, D-NH and NNH protons are deshielded and shifted to higher chemical shift values due to intramolecular hydrogen bonding shown in **figure 1.** This is validated by the broad H^+ resonance that appears around 11.56 ppm in **figure 4** upon acid-catalyzed deprotection. These hydrogen bonds may play a role in stabilizing the flattened conformation of

the macrocycle. Most importantly, this shift in resonances corroborates the belief that this macrocycle adopts a b-sheet like structure.

The spectra of **I-I** above can be assigned more readily if a COSY experiment is performed. In **Figure 5** below, the ^{1}H NMR spectrum of **I-I** is plotted against itself in two dimensions, where the same peaks are displayed on the diagonal. Cross peaks indicate which hydrogens are coupled to each other. The signals displayed are only between hydrogens on adjacent carbons, thereby allowing us to make conclusive proton assignments.

Based on the structure of **I-I**, obvious signals can be observed in the COSY. For example, D-NH (7.80 ppm) and D (2.84 ppm) should be coupled to each other. This is corroborated by the COSY and shown with red lines. Further, the β and γ_2 protons of isoleucine also show a cross peak. The protons of the acetal group (A, B, C, D) can also be assigned after A is identified. As to be expected, proton A has connectivity to B, and protons C and D also exhibit a signal. All other protons in the structure can be assigned similarly.

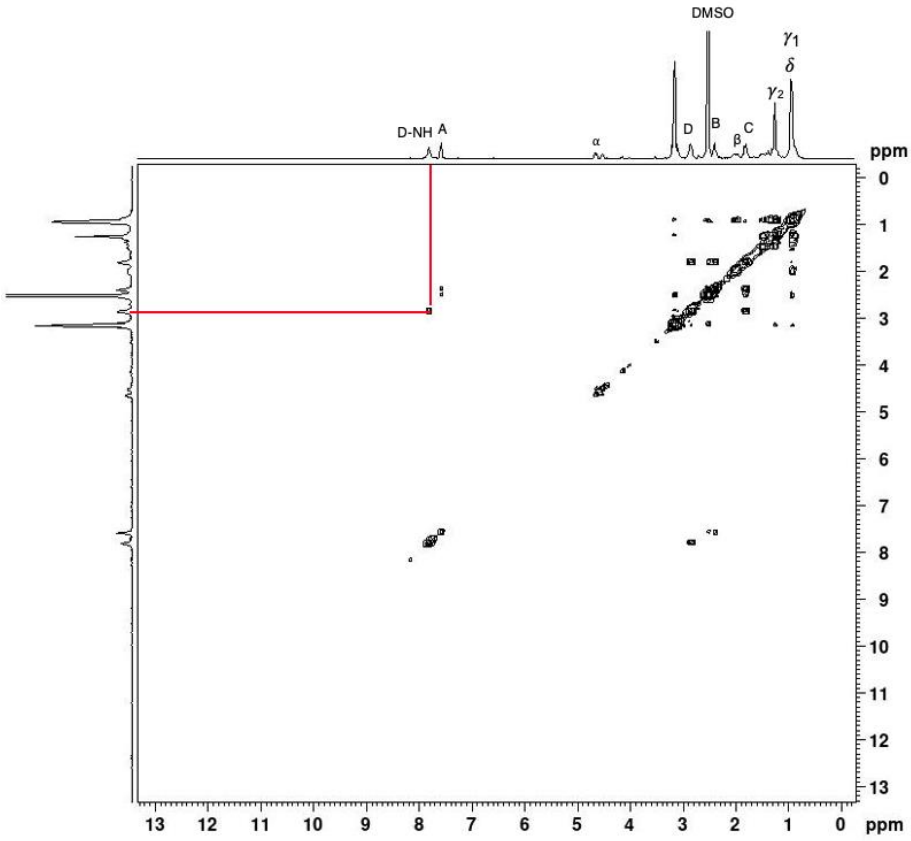

Figure 5. ^{1}H-^{1}H COSY spectrum of the macrocycle **I-I**, in DMSO-d_6. The red lines represent the signal between D-NH (7.80 ppm) and D (2.84 ppm).

The ^{13}C NMR in **figure 6** also confirms the synthesis of **I-I.** There around no peaks 90-110 ppm that represent the carbon of the diethylacetal group (-H<u>C</u>(OCH_2CH_3)$_2$). Further, the carbon of the α proton of isoleucine present just before 60 ppm. At around 140 ppm, the A carbon appears (H<u>C</u>=N).

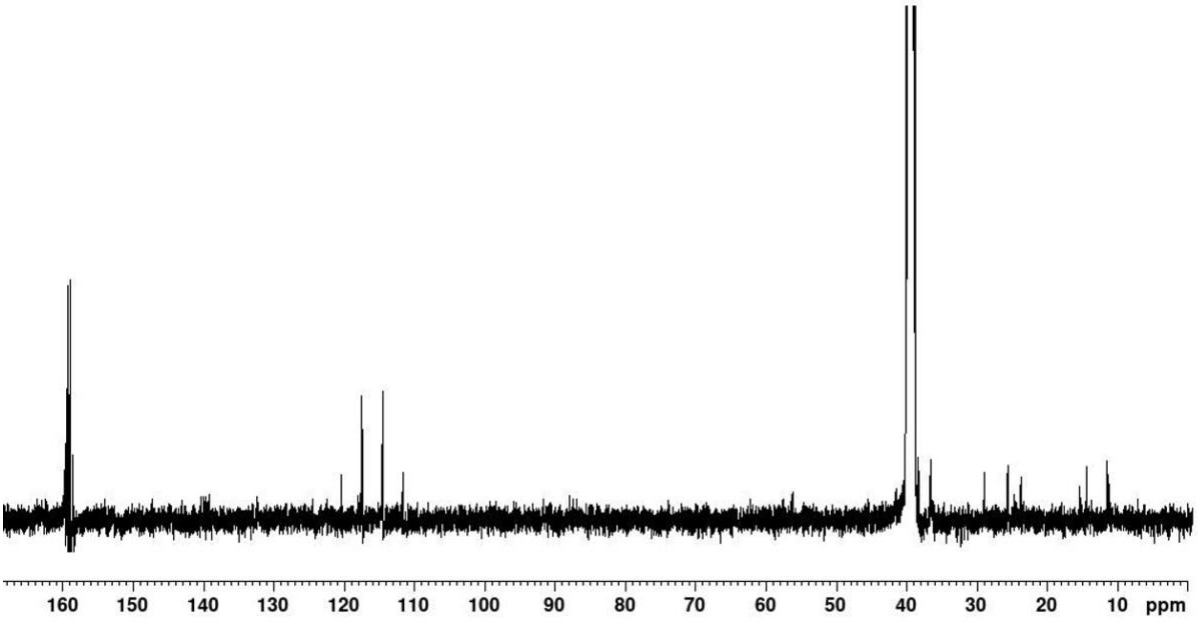

Figure 6. The 100 MHz ^{13}C NMR spectrum of **I-I** in DMSO-d_6.

Part III. Synthesis and Characterization of Heterodimer Macrocycle

***I-M** Macrocycle.* Equal molar concentrations of **I** and **M** were added to a 1:1 mixture of DCM:TFA and evaporated to dryness. The ^{1}H NMR spectra shows unique resonances that indicate heterodimer synthesis (**Figure 8).** A more prominent H+ resonance appears at 11.5 ppm and new α-NH and D-NH peaks appear at 8.9 and 8.5 ppm. Further, while the presence of two α peaks is consistent in **I-I** and **M-M**, **I-M** exhibits new α peaks at 4.1 and 4.0 ppm. The peaks in **figure 7a**

and **7b** can be assigned with ease using the COSY spectrum of **I-M** (**figure 8).** Obvious signals that are proof of synthesis are shown with red (D-NH to D) and blue lines (α-NH to α).

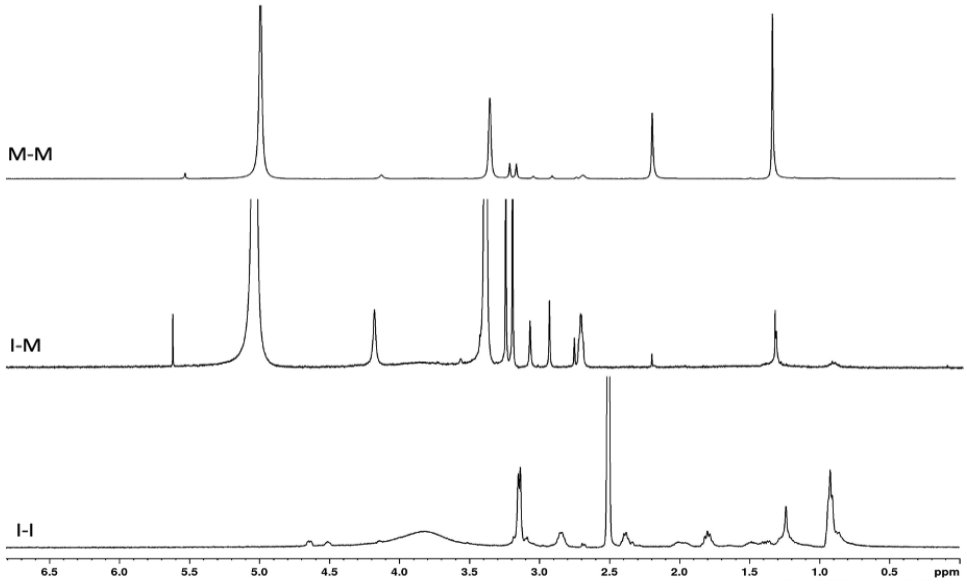

Figure 7a. The 400 MHz stacked plot ^{1}H NMR spectra of **M-M, I-M,** and **I-I** in DMSO-d_6 from 0 to 7 ppm.

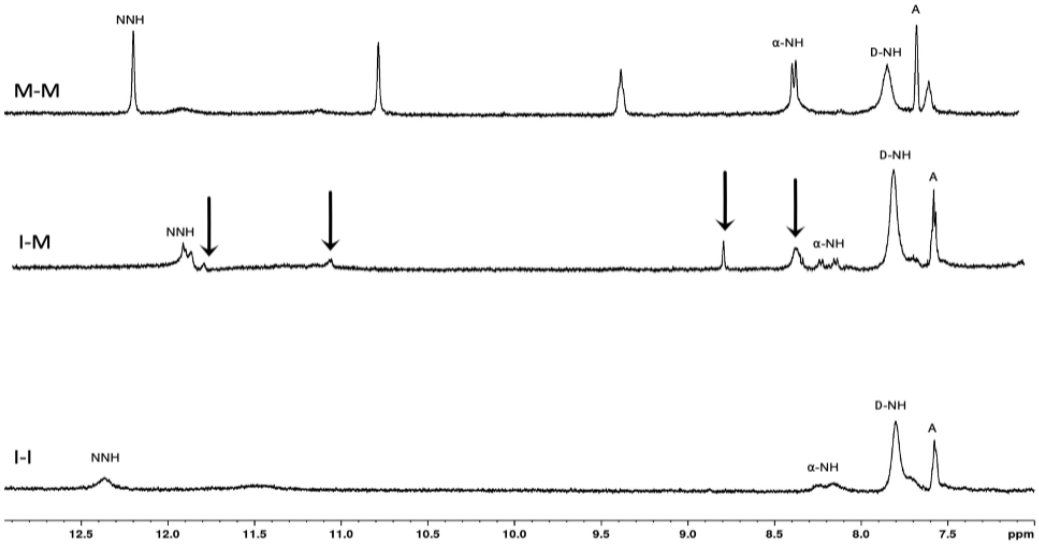

Figure 7b. The 400 MHz stacked plot ^{1}H NMR spectra of **M-M, I-M,** and **I-I** in DMSO-d_6 from 7to 13 ppm. The arrows indicate the presence of new resonances unique to the heterodimer **I-M.**

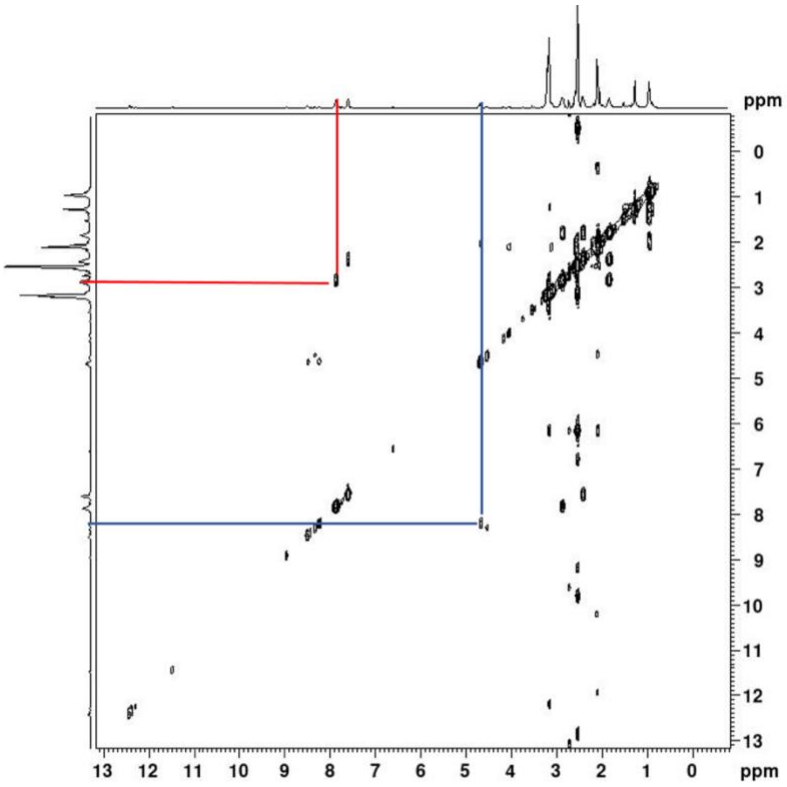

Figure 8. The ^{1}H-^{1}H COSY spectrum of heterodimer **I-M,** in DMSO-d_6. The red lines represent the signal between D-NH (7.80 ppm) and D (2.83 ppm). The blue lines represent the signal between α-NH signal (8.28 ppm) and α (4.66 ppm).

Part IV. Probing Solution Structure of Macrocycles

In an attempt to understand the solution structure of **I-I,** a 2D NMR experiment called a rOesy is performed. Each cross-peak in figures **10** and **11** correspond to a pair of protons that are in close spatial proximity thus providing information about the 3D shape of the molecule. A rOesy was obtained for **I-I** (**figure 10)**. This spectrum establishes the stereochemistry of the hydrazone due to the correlation between A and NNH. The orientation of the double bond is *E*. Further, because there is a lack of a correlation between A and DMA, it is unlikely that the macrocycle adopts a folded morphology like its 24-atom analog.

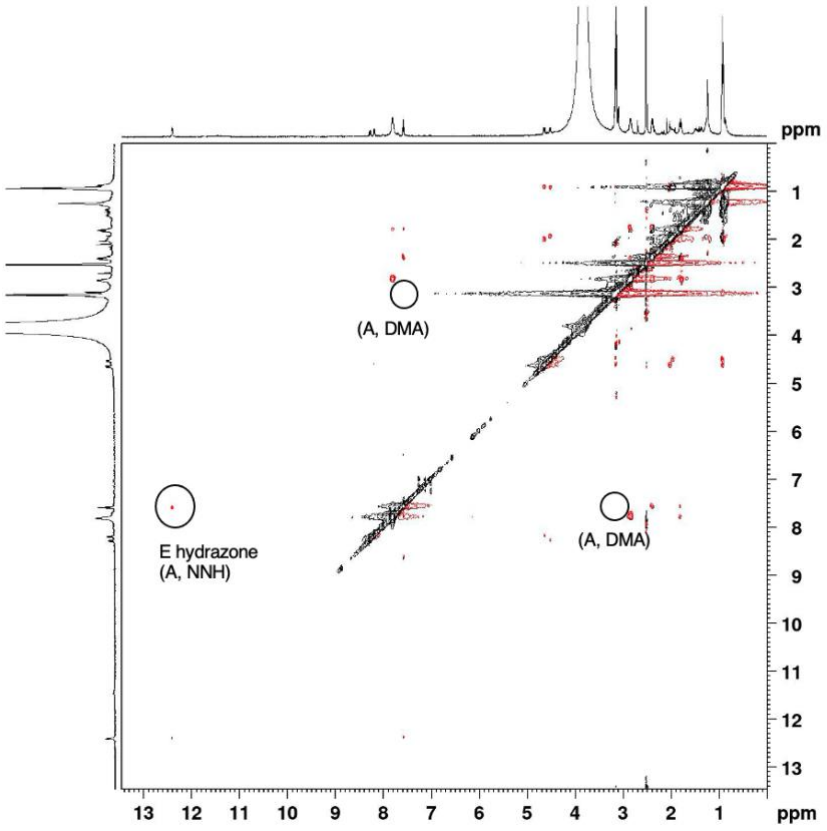

Figure 9. The rOsey NMR spectrum of **I-I** in DMSO-d_6, suggests a flat, extended structure due to missing correlation between A and DMA and an *E*-hydrazone is observed (A, NNH).

The rOesy for **I-M** is less conclusive (**figure 11).** The stereochemistry of the hydrazone cannot be concluded because of the absence of the (A, NNH) correlation. The absence of a signal between A and DMA can be noted, however. While this is not corroborating evidence, it seems likely that **I-M** also adopts a planar conformation similar to **I-I.**

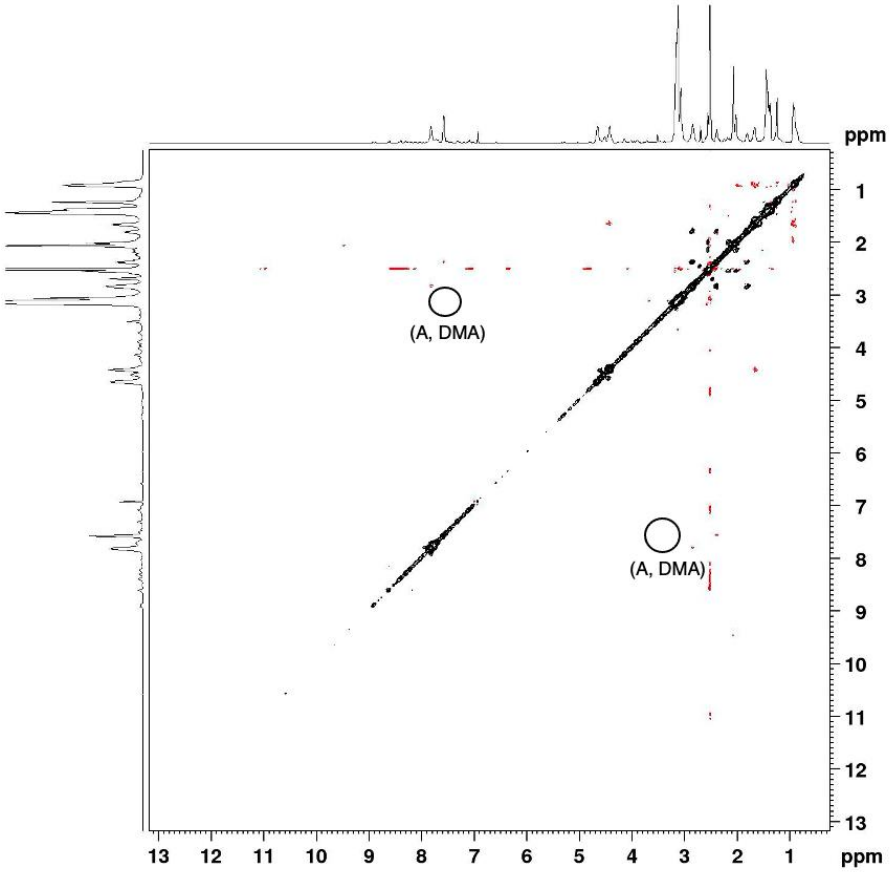

Figure 10. The rOsey NMR spectrum of **I-M** in DMSO-d_6, suggests a flat, extended structure due to missing correlation between A and DMA.

CONCLUSION

A three-step synthetic route can be used to afford **I-I**. The route for preparation involves a step-wise synthesis of a triazine core with an amino acid, hydrazine protecting group and auxiliary group (dimethylamine) to yield 43% of **I-acid.** This intermediate is then subjected to amide coupling using HBTU and a four-carbon acetal group is installed at a 34% yield. Acetal length is a carefully considered factor in this research; previous research shows different ring sizes drive the conformational flexibility of the macrocycle. The 26-atom macrocycle adopts an extended, flat state instead of a folded conformation seen in the 24-atom analog. Following amide coupling,

spontaneous dimerization with acid yields **I-I** and heterodimer **I-M.** 1D and 2D NMR spectra in DMSO-d_6 are utilized to verify successful synthesis and probe 3D confirmation of the macrocycles. The downfield shift of resonances of **I-I** in **figure 4** due to intramolecular hydrogen bonding reveals information about the conformation of this macrocycle. A network of hydrogen bonds present within the macrocycle likely stabilize the flattened, extended conformation of the macrocycle that resembles a β-sheet. Further, a network of rOe is used to reveal the stereochemistry of the *E*-hydrazone in **I-I** and support the flat, extended conformation both macrocycles likely adopt.

The successful synthesis of two macrocycles containing a 4-carbon acetal is useful in understanding how to create a scaffold that serves as a β-sheet mimic. In future research, an array of different amino acids and auxiliary groups can be incorporated to confirm that 26-atom ring sizes maintain an unfolded conformation in solution (2D-NMR techniques) and solid-state (x-ray structure) across a variety of structural modifications. These findings will help comment on how to more carefully control the topological arrangement (i.e., folded vs unfolded) of the target macrocycle, rendering the synthesis of β-sheet-like scaffolds possible.

REFERENCES

1. Dougherty, P.G.; Qian, Z.; Pei, D. Macrocycles as Protein-protein Interaction Inhibitors. *Biochem J*. **2017**, 474(7), 1109-1125. https://www.ncbi.nlm.nih.gov/pmc/articles/PMC6511976/

2. Lu, H.; Zhou, Q.; He, J. *et al.* Recent Advances in the Development of Protein-protein Interaction Modulators: Mechanisms and Clinical Trials. *S Transduct Target Ther*. **2020,** 213(5). https://doi.org/10.1038/s41392-020-00315-3

3. Jiang, Y.; Long, H.; Zhu, Y.; Zeng,Y. Macrocyclic Peptides as Regulators of Protein-protein Interactions. *Chinese Chem. Lett.* **2018,** 29(7), 1067-1073. https://doi.org/10.1016/j.cclet.2018.05.028.

4. Menke, A.J.; Gloor, C.J.; Claton, L.E.; Mekhail, M. A.; Pan, H.; Stewart, M.D.; Green, K.N.; Reibenspies, J.H.; Pavan, G.M.; Capelli, R.; Simanek, E.E. A Model for the Rapid Assessment of Solution Structures for 24-Atom Macrocycles: The Impact of β-Branched Amino Acids on Conformation. *J. Org. Chem.* **2023**, 88(5), 2692–2702. https://doi.org/10.1021/acs.joc.2c01984

5. Jimenez, D.G, Poongavanam, v, Kihlberg, J. Macrocycles in Drug Discovery – Learning from the past for the Future. *J. Med. Chem.* **2023**, 66(8), 5377–5396. https://doi.org/10.1021/acs.jmedchem.3c00134

6. Sindhikara, D.; Wagner M.; Gkeka, P.; Güssregen, S.; Tiwari, G.; Hessler, G.; Yapici, E.; Li, Z.; Evers, A. Automated Design of Macrocycles for Therapeutic Applications: From Small Molecules to Peptides and Proteins. *J. Med. Chem.* **2020**, 63(20) 12100–12115. https://doi.org/10.1021/acs.jmedchem.0c01500

7. Mallinson, J.; Collins, I. Macrocycles in New Drug Discovery. *Future Med. Chem*.

2012, 4(11), 1409–1438. https://doi.org/10.4155/fmc.12.93

8. Cheng, PN.; Liu, C.; Zhao, M. *et al.* Amyloid β-sheet mimics that antagonize protein aggregation and reduce amyloid toxicity. *Nature Chem*, **2012,** 4, 927–933. https://doi.org/10.1038/nchem.1433

9. Zheng J.; Liu, C.; Sawaya, M.R.; Vadla, B.; Khan, S.; Woods R.J.; Eisenberg, D.; Goux, W.J.; Nowick. J.S. Macrocyclic β-Sheet Peptides That Inhibit the Aggregation of a Tau-Protein-Derived Hexapeptide. *J. Am. Chem. Soc.* **2011**, 133(9), 3144–315. https://doi.org/10.1021/ja110545h

10. Baig, M.H.; Ahmad, K.; Saeed, M.; Alharbi, A.M.; Barreto, G.E.; Ashraf, G.M.; Choi, I. Peptide based therapeutics and their use for the treatment of neurodegenerative and other diseases. *J. Biopharma.* **2018**, 103, 574-581. https://doi.org/10.1016/j.biopha.2018.04.025

11. Sharma, V. R.; Mehmood, A.; Janesko, B. G.; Simanek, E. E. Efficient Syntheses of Macrocycles Ranging from 22-28 Atoms through Spontaneous Dimerization to Yield Bis-Hydrazones. *RSC Adv.* **2020**, 10(6), 3217-33220. https://doi.org/10.1039/C9RA08056B

12. Menke, A.J.; Henderson, N.C.; Kouretas, L.C.; Estenson, A.N.; Janesko, B.G.;

Simanek, E.E. Computational and Experimental Evidence for Templated Macrocyclization: The Role of a Hydrogen Bond Network in the Quantitative Dimerization of 24-Atom Macrocycles. *Molecules* **2023**, 28(3), 1144. https://doi.org/10.3390/molecules28031144

13. Cheng, P.; Pham, J.D.; Nowick. The Supramolecular Chemistry of β-Sheets. *J. Am. Chem. Soc* **2013**, 135(15), 5477-5492. https://doi.org/10.1021/ja3088407

14. Chatterjee, J.; Gilon, C.; Hoffman, A.; Kessler, H. N-Methylation of Peptides: A New Perspective in Medicinal Chemistry. *Acc. Chem. Res*. **2008**, 41(10), 1331-1342. https://doi.org/10.1021/ar8000603

15. Stocker, M. Two-Dimensional (2D) Solid-State NMR Spectroscopy. *Studies in Surf. Sci. Cat.* **1994,** 85, 429-507. https://doi.org/10.1016/S0167-2991(08)60776-4.

16. Raju, M.; Maeorg, S.; Tsubrik, O.; Maeorg, U.; Efficient solventless technique for Boc-protection of hydrazines and amines. *ARKIVOC.* **2009,** 2009(6), 291-297. http://dx.doi.org/10.3998/ark.5550190.0010.628